Charge-density study of the nonlinear optical precursor DED-TCNQ at 20 K

Jacqueline M. Cole*
Institut Laue Langevin, B.P. 156, 38042 Grenoble Cedex 9, France;
Department of Chemistry, University of Durham, South Road, Durham DH1 3LE, United Kingdom;
and Department of Chemistry, University of Cambridge, Lensfield Road, Cambridge CB2 1EW, United Kingdom

Royston C. B. Copley†
Department of Chemistry, University of Durham, South Road, Durham DH1 3LE, United Kingdom

Garry J. McIntyre
Institut Laue Langevin, B.P. 156, 38042 Grenoble Cedex 9, France

Judith A. K. Howard
Department of Chemistry, University of Durham, South Road, Durham DH1 3LE, United Kingdom

Marek Szablewski and Graham H. Cross
Department of Physics, University of Durham, South Road, Durham DH1 3LE, United Kingdom
(Received 29 November 2000; revised manuscript received 24 May 2001; published 13 March 2002)

A charge-density study of the nonlinear-optical (NLO) precursor {4-[bis(diethylamino)-methylium] phenyl}dicyanomethanide (DED-TCNQ), space group $P2_1/c$, $a=11.174(2)$ Å; $b=12.859(2)$ Å; $c=12.486(2)$ Å; $\beta=112.00(1)°$, is presented. The results derive from a suitable combination of complementary 20 K x-ray and neutron diffraction data, the latter being important for locating the hydrogen atoms precisely. The compound is one in a series of TCNQ derivatives that exhibit varying degrees of quinoidal and zwitterionic character, these two electronic states being very close energetically. Bond-length-alternation type calculations show that the molecule at 20 K exists in a mixture of the two states, the zwitterionic ground state being dominant (63:37% zwitterionic: quinoidal). A topological analysis of the bonding density within the benzenoid ring provides for a more direct, alternative method to calculate this ratio which utilizes ellipticity values derived from the charge-density study. Results are identical thus corroborating the validity of the ''strength-length'' relationship implicitly assumed in bond-length-alternation type calculations. The ratio determined corresponds well to the electronic configuration needed to meet the requirements of the general rule for obtaining a maximum value of β (a measure of the NLO response on the molecular scale) as a function of bond-length alternation. The promise of this class of compounds for nonlinear optics also lies partly in their high molecular dipole moments and so the pseudoatomic charges derived from this study were used to evaluate the nature of the molecular charge transfer in detail and the solid-state dipolar vector moment μ. Such measurements of μ are otherwise difficult in the solid state. A value of $|\mu|=91\times10^{-30}$ Cm was deduced which compares with liquid and gas phase theoretical calculations of $\mu=66.71\times10^{-30}$ Cm and $\mu=33.36\times10^{-30}$ Cm, respectively. This comparison, combined with an analysis of the sense of this vector, show that local crystal-field effects are highly influential in the solid state.

DOI: 10.1103/PhysRevB.65.125107 PACS number(s): 61.10.−i, 61.12.−q, 42.65.−k

I. INTRODUCTION

Highly dipolar tetracyano-*p*-quinodimethane (TCNQ) derivatives have shown considerable potential as second-order nonlinear-optical (NLO) precursors on account of their desirable structural attributes.[1–5] On a molecular scale, high levels of charge-transfer and significant transition-state dipole moments are known to lead to good second-order NLO activity in organic materials. The well-known charge-transfer properties of TCNQ adducts, coupled with the fact that two energetically close electronic configurations (zwitterionic and quinoidal—see Fig. 1) constitute the overall ground-state of these compounds, are the primary sources of their NLO behavior.

The relative balance between zwitterionic and quinoidal character that exists in these materials is particularly important given bond-length-alternation (BLA) considerations: BLA, defined as the average of the difference in length between adjacent C-C bonds in a conjugated chain, has been shown to largely control the value of the molecular hyperpolarizability β, a measure of the second-order NLO effect on the molecular scale.[6,7] As a general rule, a small value of BLA, corresponding to a electronic configuration lying halfway between the fully delocalized state (cyanine limit) and either the zwitterionic or quinoidal state, yields the largest β coefficient and thus good NLO activity. Figure 1 illustrates the general profile of this trend; such generality should be emphasized since the diagram is representative of an idealized conjugated chain[8] and so a plot specific to the more complex molecules presented below the graph would naturally be more complicated than this simplified model.

The negative solvatochromatic behavior observed in

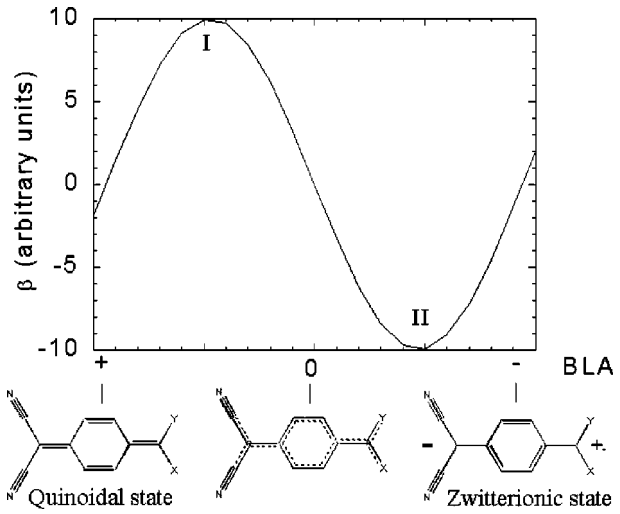

FIG. 1. The general profile of the first hyperpolarizability coefficient β as a function of BLA. Note that the plot represents a generic one but its derivation is based on known principles obtained from theoretical studies of the influence of BLA on β for a polyene system (Ref. 8). In such studies, β is defined as being negative where negative BLA is observed; however, this is simply a matter of definition as the measurable value of β can of course be only positive or null and thus the points I and II both represent local *maxima* of β.

many of the TCNQ derivatives hitherto studied, including the subject compound {4-[bis(diethylamino)-methylium]phenyl}dicyanomethanide (DED-TCNQ),[2] indicates that the electronic configuration of the subject compound resembles more closely the zwitterionic form rather than the quinoidal neutral state, i.e., the value of β lies on a point on the right-hand-side of the graph in Fig. 1. A substantial mix of the two states has been deduced from previous BLA-type studies.[2] Thus, the compound possesses a low value of BLA, i.e., a β value close to the minimum point (maximum negative β) depicted in Fig. 1.

The highly dipolar nature of these species is also important for second-order NLO properties, since

$$\beta \propto \left(\frac{\mu_{ee}^2(\mu_{ee}-\mu_{gg})}{E_{ge}^2} \right) \tag{1}$$

if we assume that a two-level model[9–11] is valid, which is reasonable here given the closely planar nature of these compounds. Suffixes *e* and *g* represent excited and ground states, respectively.

The large values of μ typically present in this class of compounds usually force the molecules to pack centrosymmetrically in a crystalline environment since the dipolar charges oppose each other in close proximity. However, the presence of noncentrosymmetry is a prerequisite for the observation of second-order NLO effects on the bulk scale, since β and $\chi^{(2)}$ are third-rank tensors.[12] Second-order NLO properties are, therefore, not observed in such compounds in the solid-state without the aid of an inert host matrix to suitably align the molecules in a head-to-tail fashion such that this crystalline symmetry restriction is overcome.

As a consequence, electric field-induced second harmonic generation (EFISH) and hyper-Raleigh scattering (HRS) measurements of such compounds in solution are utilized to determine the static hyperpolarizability β. EFISH measurements have, however, proved problematic for this series of compounds due to the finite optical absorption at 532 nm and the problems of aggregation at the concentrations required for this technique.[13] On the other hand, HRS measurements have proved successful and yield values of $\beta(0)$ (the zero frequency value) of the order 3×10^{-28} esu (Ref. 4).

Although the molecular structure of target compounds whilst in an inert matrix or in solution can only be realized with limited detail, single-crystal diffraction techniques can provide a wealth of information regarding the molecular structure, albeit within a crystalline framework. Moreover, a comparison of the crystal state molecular polarization with free-state or solution-state polarization, deduced from complementary theoretical studies is also important, since it could provide a valuable insight into local-field effects that ensue, these being of direct consequence on the macroscopic NLO response of a material since for second-harmonic generation

$$\chi^{(2)} = N f_I^{2\omega} f_J^{\omega} f_K^{\omega} \langle \beta_{ijk} \rangle_{IJK}, \tag{2}$$

where N is the number of molecules per unit volume, f_x are the local field factors in the crystal frame *IJK* at the fundamental and second harmonic frequencies, ω and 2ω, respectively, and $\langle \beta_{ijk} \rangle_{IJK}$ is the expectation value of β_{ijk}, i.e., the weighted sum of β in the molecular frame *ijk* over all orientations of a given molecule, with respect to the crystal frame.[14,15]

A charge-density study on DED-TCNQ was conducted since this methodology enables one to realize the most detailed and subtle structural features existing in the molecule thus allowing us to investigate the nature of BLA effects in detail which is important since they directly affect β: see Fig. 1. Such a study is not only superior to a conventional crystallographic refinement, that uses the independent atom model (IAM) formalism, on account of the ability to model the bonding density much better, but also, the IAM implicitly assumes no atomic charge. This renders such refinements inadequate for detailed bonding analysis particularly when high levels of polarization and thus charge-transfer effects prevail, as in nonlinear-optical compounds and their precursors. Furthermore, an additional advantage of incorporating such charges in the structural model of these materials is that an experimental value of the solid-state dipole moment can be deduced. The evaluation of such a parameter in this phase is difficult by any other means and it is particularly important to deduce this value for NLO materials and precursors since β is highly dependent on μ [see Eq. (1)]. The fact that the subject material is SHG active, while the molecules are in an inert matrix or in solution, makes this parameterization of μ in the solid-state even more pertinent since its comparison with calculated gas and liquid phase μ values provides important information for assessing the extent of local-field effects. Such effects have a direct bearing on the relationship between molecular (β) and macroscopic ($\chi^{(2)}$) measures of

the second-order NLO output [see Eq. (2)]. The subject compound DED-TCNQ was chosen since it represents one of the most promising candidates for NLO application in the TCNQ series studied thus far, on account of its low BLA value and dominating zwitterionic character.

II. EXPERIMENTAL

A. Synthesis

DED-TCNQ was prepared by the reaction of TCNQ with *N, N* diethylamine in THF by methods analogous to those described by Hertler and co-workers.[16] Single-crystals were grown from acetonitrile solution.

B. Charge-density measurements

1. Single-crystal x-ray diffraction

A $0.24\times0.24\times0.14$ mm crystal of DED-TCNQ was centered on the *Fddd* cryodiffractometer at Durham, UK,[17] a device equipped with a Mo rotating anode ($\lambda = 0.71073$ Å), thus enabling data collection of weak or small samples and incorporating subliquid nitrogen temperature measurement capabilities via an Air Products 512 Displex. The crystal was cooled at 0.75 K min^{-1} to 150 K and then at 0.14 K min^{-1} to 20.0(1) K, the latter being the temperature of all intensity measurements. The very low temperature of data-collection is important for yielding the maximum possible intensity of atomic scattering, $(\sin\theta/\lambda)_{max}$ being of paramount concern in charge-density studies since the high-angle (weaker) data represent mostly the atomic scattering from the core electrons, thus making possible a multipolar refinement of the structural data. It also enables the largest number of reflections to be observed which is important since the multipolar refinement introduces a large number of parameters.

The cell parameters were obtained initially using 24 reflections in the range $22.15°\leqslant 2\theta\leqslant 23.92°$ and refined subsequently using all low-angle ($<50°$) data. Data were collected in bisecting mode using $2\theta/\omega$ scans, the scan width being set from 1.3° in 2θ below K-α_1 to 1.6° in 2θ above K-α_2, and a constant scan speed of 6° in 2θ per minute was employed. A sphere of data was collected out to $2\theta=50°$ as was a nearly complete hemispherical shell out to $2\theta=95°$. This totaled 41 407 reflections over a period of one month. Seven standard reflections were measured every 193 reflections except in the range 80–95° in 2θ, where only five could be reached due to the restricted angular range of the χ circle. No absorption correction was necessary due to the small size of the crystal and the small value of the absorption coefficient.

Several small areas of reciprocal space were contaminated by the presence of powder lines from the graphite pin used to mount the crystal. The corresponding data (totalling 331 reflections) were located using Crystal Logics software and a local program, and removed from the resulting data-set without adverse effect since redundancy was high and these data represent under 0.01% of the total reflections collected. The data were reduced using a local program based on Lehmann and Larsen[18] and the DREAM suite of programs.[19] The resulting scaled and merged data yielded an R_{int} of 0.0272. A summary of crystal and data collection parameters is given in Table I.

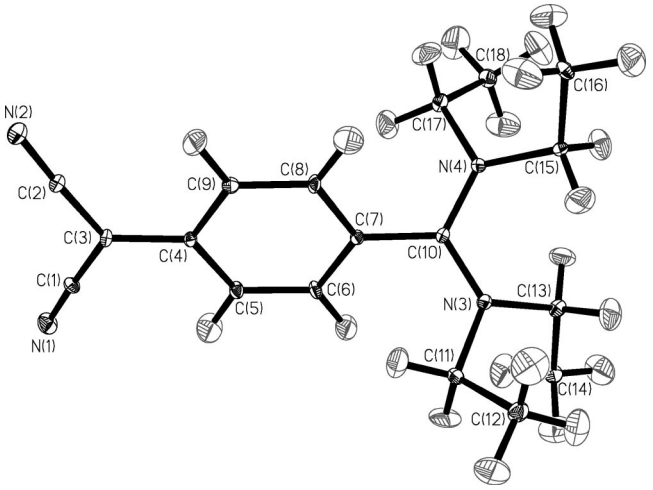

FIG. 2. A 50% probability thermal ellipsoid plot of the 20 K neutron structure of DED-TCNQ.

2. Single-crystal neutron diffraction

A $1.0\times1.0\times1.0$ mm crystal of DED-TCNQ was centered on the four-circle diffractometer *D*9, at the Institut Laue Langevin (ILL), Grenoble, France. Indexing and subsequent data collection was carried out at 20.0(1) K using Cu (220) monochromated neutron radiation [$\lambda=0.8417(2)$ Å]. Half-wavelength contamination was removed with an erbium filter. The low temperature, employed to minimize possible diminution of scattering due to thermal effects, was maintained using an Air Products 512 displex. 3443 unique reflections ($1°<2\theta<70°$) were measured according to a ω-$x\theta$ scanning procedure, with x chosen to keep the reflection in the middle of the detector aperture and with a scan width $\Delta\omega$, which was roughly twice the full width of the peak at background level. A standard reflection, measured every 50 reflections, showed no variation in intensity. Data were reduced using a local program[20] and Lorentz corrections were applied. Absorption corrections were made by Gaussian integration[21] using the calculated attenuation coefficient $\mu = 0.21$ mm^{-1} to give a transmission range 0.779–0.846. The merged data yielded $R_{int}=0.0583$. The structure was refined by full-matrix least-squares refinement using SHELXL-93 (Ref. 22) against 3417 reflections. Atomic positional and anisotropic displacement parameters for all atoms were refined and a 50% probability thermal ellipsoid plot of the neutron derived structure is given in Fig. 2. Table I provides a summary of all relevant crystal, data collection and refinement parameters.

C. Multipolar refinement

Initial atomic coordinates and thermal parameters were taken from a conventional Independent Atom Model (IAM) refinement of the x-ray data, using SHELXL-93 (Ref. 22) (see Table I). Multipolar refinement was applied to this model

TABLE I. A summary of crystal, data collection, and IAM refinement parameters for the 20 K x-ray and neutron structure of DED-TCNQ.

Parameter	20 K x-ray (IAM) study	20 K neutron (IAM) study
Molecular formula	$C_{18}H_{24}N_4$	$C_{18}H_{24}N_4$
Formula weight	296.41	296.41
a(Å)	11.174(2)	11.178(1)[a]
b(Å)	12.859(2)	12.859(1)[a]
c(Å)	12.486(2)	12.476(1)[a]
α(°)	90	90
β(°)	112.00(1)	112.044(5)[a]
γ(°)	90	90
Cell volume (Å^3)	1663.4(5)	1662.2(4)[a]
Crystal system	monoclinic	monoclinic
Space group	$P2(1)/c$	$P2(1)/c$
Z	4	4
Calculated density (g cm^{-1})	1.184	1.182
Temperature (K)	20.0(1)	20.0(2)
Wavelength (Å)	0.71073	0.8417(2)
Absorption coefficient (mm^{-1})	0.072	0.2137
Crystal morphology	rectangular	cubic
Crystal color	yellowy-brown	yellowy-brown
Crystal size (mm)	0.24×0.24×0.14	1.0×1.0×1.0
Total number of reflections	41407	3773
Unique reflections	14919	3443
Observed reflections [$I>2\sigma(I)$]	8562	2184
R_{int}	0.0272	0.0583
$(\sin\theta/\lambda)_{\max}$	1.037	0.681
Data/parameters	14907/295	3417/415
$R(F)[I>2\sigma(I)]$	0.0604	0.0532
$R(F^2)[I>2\sigma(I)]$	0.1018	0.0890
GOF$_w$	1.123	1.330
Weighting scheme	$1/\sigma^2$	$1/\sigma^2$
$\Delta\rho_{(\max,\min)}$	0.720/−0.447e Å^{-3}	1.108/−1.096 fm Å^{-3}

[a]Although these cell parameters are neutron derived, the 20 K x-ray determined cell parameters $a=11.174(2)$ Å, $b=12.859(2)$ Å, $c=12.486(2)$ Å, $\beta=112.00(1)°$ were used in all correction and refinement procedures since they are deemed more accurate than neutron derived values, as is usual. Moreover, the estimated standard deviation of the neutron wavelength was not used in the calculation of the neutron derived cell parameters:

$$R(F)=\frac{\Sigma\|F_0|-|F_c\|}{\Sigma|F_0|};\quad R_w(F^2)=\left[\frac{\Sigma[w(F_0^2-F_c^2)^2]}{\Sigma[w(F_0^2)^2]}\right]^{1/2};\quad \text{GOF}=\left[\frac{\Sigma[w(F_0^2-F_c^2)^2]}{n-p}\right]^{1/2};\quad R_{\text{int}}=\frac{\Sigma|F_0^2-F_0^2(\text{mean})|}{\Sigma F_0^2}.$$

using the XD suite of programs.[23] This employs spherical and aspherical atom-centred density functions to model the total electron density of the structure in the following manner:

$$\rho_{\text{atom}}(\mathbf{r})=P_c\rho_{\text{core}}(r)+P_v\kappa^3\rho_{\text{valence}}(\kappa r)+\sum_{l=0}^{l_{\max}}\kappa'^3R_l(\kappa' r)\sum_{m=0}^{l}P_{l\text{m},\pm}d_{l\text{m},\pm}(\mathbf{r}/r),\quad (3)$$

where ρ_{core} and ρ_{valence} are Hartree-Fock spherical core and valence densities, respectively, P_c and P_v are the populations of the core and valence shells, respectively, $P_{1m\pm}$ are the multipolar population parameters of each normalized associated Legendre function $d_{lm\pm}$ of order l [monopolar ($l=0$), dipolar ($l=1$), quadrupolar ($l=2$), octopolar ($l=3$), hexadecapolar ($l=4$)], m corresponds to the orientation of l, κ and κ' are the contraction-expansion coefficients for the spherical and multipolar valence densities, respectively, and $R_l(\kappa' r)$ represents the Slater-type radial functions as defined by

$$R_l(r)=[(\xi^{n_1+3})/(n_l+2)!](r)^{n(l)}\exp(-\xi r),\quad (4)$$

where $n>1$ is required to satisfy Poisson's electrostatic requirements[24] and ξ is the energy-optimized single Slater orbital exponent for the electron subshells of isolated atoms $\xi=(Z\text{-}\sigma)/n$ (Z=charge, σ=screening constant, n

TABLE II. A summary of refinement parameters for the charge density study of DED-TCNQ.

Parameter	Value	Parameter	Value
Scale Factor	0.2480(6)	Weighting scheme	$1/\sigma^2$
Criterion for observed data	$F=2\sigma(F)$	$R_w(F)$	0.0400
$R(F)$	0.0474	$R_w(F^2)$	0.0713
$R(F^2)$	0.0517	GOF_w	1.1666
$R_{\mathrm{all}}(F)$	0.1566	Data/parameter	6537/609
$R_{\mathrm{all}}(F^2)$	0.0819	$\Delta/\sigma_{(\mathrm{min/max})}$	$2.1\times10^{-9}/3.2\times10^{-5}$
GOF	1.1042	$\Delta\rho_{(\mathrm{min/max})}$	$-0.190/0.097$ eÅ^{-3}

=principal quantum number) and for each element it is taken from tabulated values[25] and modified by the variable κ', such that $\xi'=\kappa'\xi$ (Ref. 26).

Once the refinement of the initial parameters had converged, a κ parameter for each atom was introduced. All κ values relating to nonhydrogen atoms were initially set at 1.0 and refined whereas the κ value for hydrogen atoms was fixed to the Stewart-Davidson-Simpson[27] (SDS) value of 1.16. The hydrogen coordinates and anisotropic displacement parameters in the XD refinement were then replaced by the refined neutron derived values. While the coordinates directly replaced the x-ray derived ones, the neutron hydrogen thermal parameters had to be scaled with respect to the x-ray ones before substitution. The scaling parameter was determined from the difference between the x-ray and neutron nonhydrogen anisotropic displacement parameters according to the weighted formula by Blessing[28]

$$U_{X^{ij}}=U_{N^{ij}}+\Delta U^{ij}, \tag{5}$$

where

$$\Delta U^{ij}=\sum_a\left[\sum_a wU_{X^{ij}}-\sum_a wU_{N^{ij}}\right]\Big/\sum_a w$$

and

$$w=1/\sigma^2,$$

where

$$\sigma=\sigma(U_{X^{ij}}-U_{N^{ij}})=[\sigma^2(U_{X^{ij}}+\sigma^2(U_{N^{ij}})]^{1/2}. \tag{6}$$

The scaling parameter was small $[-5.40\times10^{-4}]$, thus indicating that there is good agreement between the thermal parameters derived from the two diffraction experiments at 20 K. The scaling parameter was simply added to all hydrogen atom thermal parameters to give the substituted values. The resulting hydrogen positions and thermal parameters were fixed in all subsequent refinements.

Multipolar terms were then introduced starting with the refinement of monopoles and dipoles (bond-directed ones for hydrogen atoms) on all atoms. Once converged, quadrupolar and octopolar terms were refined for all nonhydrogen atoms. Refinement at the hexadecapolar level for all nonhydrogen atoms was also attempted. However, the population of these functions was negligible [maximum hexadecapolar function population was less than twice its estimated standard deviation] and so were not included in final refinements.

The κ parameters were then sub-divided into six values that reflected the different chemical environments of a given element. The six κ values represented the six following groups of atoms

Group 1: All *sp* hybridized nitrogen atoms [N(1) and N(2)].

Group 2: All sp^2 hybridized nitrogen atoms [N(3) and N(4)].

Group 3: All *sp* hybridized carbon atoms [C(1) and C(2)].

Group 4: All sp^2 hybridized carbon atoms [C(3) to C(10)].

Group 5: All sp^3 hybridized carbon atoms [C(11) to C(18)].

Group 6: All hydrogen atoms.

κ values for the first five groups were refined, as were the κ' parameters subsequently such that, for all of the multipoles employed, the value of κ' in each κ group was constrained to have the same value (since κ' values for each multipole are strongly correlated to each other). For group 6, both κ and κ' were fixed at the SDS value of 1.16 (see earlier).

III. RESULTS AND DISCUSSION

A summary of the multipolar refinement details is given in Table II while the bond distances from the charge-density study (the C-H distances being those taken from the neutron refinement) are provided in Table III. All nonhydrogen distances are markedly more accurate than those derived from the analogous IAM refinement, as expected. Moreover, there are significant discrepancies ($>2\sigma$) between IAM and multipole-derived bond distances in areas of notable charge transfer (e.g., the nitrile groups and benzenoid ring) thus indicating the inadequacies of the IAM for structures of such compounds. The neutron derived C-H distances are naturally much more precise than ones derived from x-ray diffraction data. Such distances were used to confirm a previous hypothesis[2] that the subject compound possesses no hydrogen bonding in the crystalline state.

A. Topological analysis of electronic structure

The topology of the charge-distribution was analyzed in the three principal areas of the molecule: the benzenoid ring,

TABLE III. Bond distances for DED-TCNQ as derived from the charge-density study.

Bond	Distance (Å)	Bond	Distance (Å)
N(1)—C(1)	1.1720(16)	C(11)—H(11*A*)	1.0840(9)
N(2)—C(2)	1.1724(15)	C(11)—H(11*B*)	1.0794(10)
N(3)—C(10)	1.3431(12)	C(12)—H(12*A*)	1.0981(11)
N(3)—C(11)	1.4773(13)	C(12)—H(12*B*)	1.0806(10)
N(3)—C(13)	1.4812(13)	C(12)—H(12*C*)	1.0870(12)
N(4)—C(10)	1.3457(12)	C(13)—C(14)	1.5275(13)
N(4)—C(15)	1.4780(13)	C(13)—H(13*A*)	1.0993(10)
N(4)—C(17)	1.4813(13)	C(13)—H(13*B*)	1.0876(10)
C(1)—C(3)	1.4100(14)	C(14)—H(14*A*)	1.0802(11)
C(2)—C(3)	1.4072(14)	C(14)—H(14*B*)	1.0793(10)
C(3)—C(4)	1.4426(12)	C(14)—H(14*C*)	1.1004(11)
C(4)—C(5)	1.4211(13)	C(15)—C(16)	1.5279(13)
C(4)—C(9)	1.4204(13)	C(15)—H(15*A*)	1.0811(10)
C(5)—C(6)	1.3886(12)	C(15)—H(15*B*)	1.0936(10)
C(5)—H(5)	1.0824(10)	C(16)—H(16*A*)	1.0962(10)
C(6)—C(7)	1.4097(13)	C(16)—H(16*B*)	1.0920(10)
C(6)—H(6)	1.0920(10)	C(16)—H(16*C*)	1.0897(11)
C(7)—C(8)	1.4080(12)	C(17)—C(18)	1.5263(14)
C(7)—C(10)	1.4673(12)	C(17)—H(17*A*)	1.0870(10)
C(8)—C(9)	1.3870(12)	C(17)—H(17*B*)	1.0816(10)
C(8)—H(8)	1.0902(10)	C(18)—H(18*A*)	1.0864(11)
C(9)—H(9)	1.0869(10)	C(18)—H(18*B*)	1.0894(11)
C(11)—C(12)	1.5247(13)	C(18)—H(18*C*)	1.0872(11)

its $-C(CN)_2$ substituent, and the *para*-substituent in the area immediately vicinal to the ring. Figure 3 shows dynamic model maps $F_{\text{multipole}}-F_{\text{spherical}}$, for the principal molecular fragments, which represent the contribution of the multipolar terms to the model. The corresponding static maps are not given here because they show very little difference since the thermal vibration in the molecule is so small. Residual density maps of the molecule, also given in Fig. 3, show featureless regions of only a little residual electron density, thus indicating that the electron distribution is well described by the multipole model. The rigid-bond test,[29] which was applied to all bonds not involving hydrogen atoms during the refinement, was satisfied throughout, all differences in the mean square displacement amplitudes (ΔMSDA) being $\leqslant 6\times10^{-4}$ Å^2 for bonds containing any π character, and $\leqslant 11\times10^{-4}$ Å^2 for those belonging to the ethyl groups, see Hirshfeld's criterion for carbon atoms $\Delta\text{MSDA}\leqslant 0.001$ Å^2.

1. Modelling of molecular charge-transfer

Since an electroneutrality constraint is applied over the whole asymmetric unit, the extent of charge transfer ensuing within the molecule can be derived wholly from the monopole populations. The charge on a given atom is the difference between the monopole population for this atom, observed from the charge-density study, and the number of valence electrons present classically in the atom, e.g., four for a carbon atom. The charges present on each nonhydrogen atom in DED-TCNQ are given in Table IV.

All values of the derived charges conform to simple electronegativity expectations. The charge-transfer properties of the molecule appear to be dominated by the nitrogen atoms, since they contain the bulk of the negative charge. This renders the entire $-C(CN)_2$ ring substituent negatively charged as one would expect for a molecule with predominantly zwitterionic character in its ground state (see Fig. 1). The complementary localization of positive charge on the carbon atoms, vicinal to N(3) and N(4), and notably on C(10) since it is common to these nitrogen atoms and adjacent to the ring, also resemble well the preponderance of the zwitterionic electronic form. The remaining negative charge is balanced principally by positive hydrogen-atom contributions, due to the electron donating nature of C-H bonds. Thus, the alkyl side chains must also play a significant role in the good level of polarization obtainable in this compound. These charge-transfer features, coupled with the null pseudoatom charges of the phenyl ring atoms within experimental error, indicate that the electronic configuration of the molecule conforms well to the idealized charge-separated donor-(*para*)-acceptor (DA) formalism, so desirable for NLO applications of organic molecules.

2. Polarization of electron density

Electron deformation density (EDD) maps for the planar parts of the molecule are given in Fig. 4. These plots show ρ-ρ_{IAM}, thus yielding a topological representation of the valence electron density distribution of the molecule. The nature and extent of the bonding and polarization ensuing in the molecule can thus be inferred. All bond $(3,-1)$ critical points and ellipticity values found within the molecule are given in Table V. Bond critical points are the point of minimum overlap between two atoms (with local maxima of electron density curvature in the orthogonal directions to the bond vector) and ellipticity ε is a measure of the amount of π bonding present in the bond: $\varepsilon=0$ pertains to no π-bonding electron density and a large value of ε denotes a substantial amount of π bonding present.[30] Note that the principal axes of the ellipse defined to measure this quantity lie perpendicular to the bond vector i.e., one is taking a cross section of the bond. Therefore, if any triple-bonding character is present in a bond, this will result in a deceptively lower value of ε than expected since the combination of double and triple bonding will make this cross section more spherical as ε tends to zero.

The EDD map in Fig. 4(a) illustrates the high level of triple-bonded character in each nitrile group. Corresponding critical points lie noticeably closer to the carbon atom than the nitrogen atom as expected and ellipticity values are small. The nitrogen lone pairs on both N(1) and N(2) can be seen clearly. Electron density in the adjoining C(1)-C(3) and C(2)-C(3) bonds appears to be polarized towards each nitrile group as expected from electronegativity arguments. Corresponding ellipticity values for these bonds and those for C(3) and C(4) are typical for a delocalized π-bonded system, thus indicating that there is a marked presence of the zwitterionic electronic configuration, its formal negative charge being delocalised fairly evenly over all bonds emanating from C(3). Such a spread of delocalization lends the molecule well to

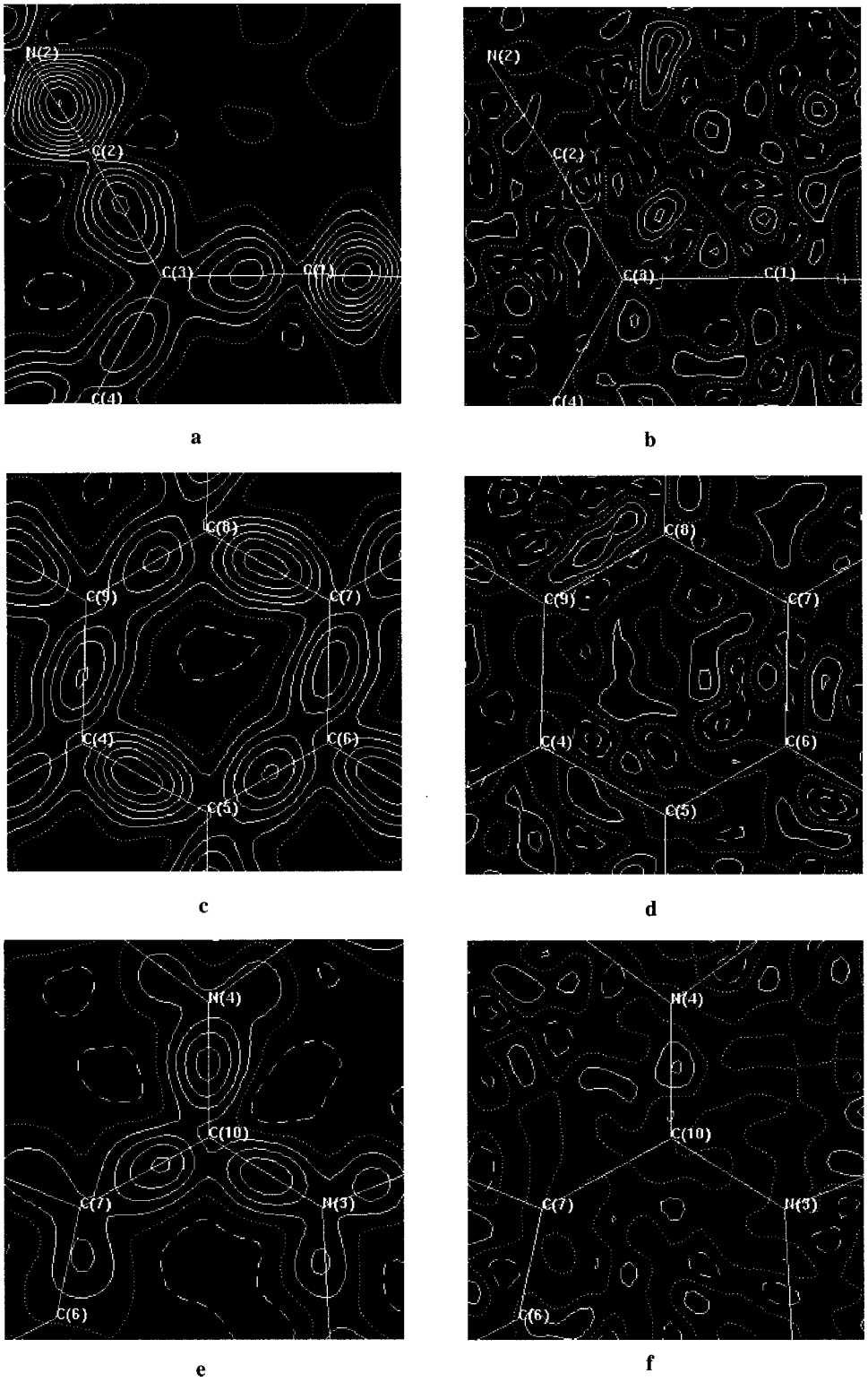

FIG. 3. Dynamic and residual maps for the (a/b) nitrile, (c/d) phenyl, (e/f) substitution point of the -C(N$Et)_2$ group in DED-TCNQ out to $\sin\theta/\lambda = 0.7$ Å^{-1} and with contour levels of 0.1 e/Å. (Solid lines are positive, dashed lines are negative, and dotted lines are zero.)

charge-transfer processes, especially since C(3) is vicinal to the phenyl ring, thereby extending the usual conjugation to the nearest neighbor of the ring from the phenyl group right through to the nitrile terminal substituents.

The EDD map of the phenyl ring [Fig. 4(b)] shows that the zwitterionic (aromatic) form is more favored over the quinoidal form, all bonds having fairly similar concentrations of electron density ($\nabla^2\rho$) and relevant ellipticity values that are typical for aromatic bonds. The ellipticity values corresponding to the bonds C(4)-C(5) and C(4)-C(9), are slightly lower than those of other bonds in the phenyl ring, but presumably, this slight diminution in π-bonding is a simply a consequence of the conjugation with the C(3) atom. All C-C bond critical points lie at the centers of each respective bond thus implying no electronic polarization within the ring. This moiety therefore acts as a *passive* medium for

TABLE IV. Pseudoatomic charges for each nonhydrogen atom in DED-TCNQ.

Atom	Charge	Atom	Charge
N(1)	−0.17(12)	C(8)	0.00(7)
N(2)	−0.20(12)	C(9)	0.00(7)
N(3)	−0.30(9)	C(10)	0.12(9)
N(4)	−0.36(9)	C(11)	0.01(8)
C(1)	−0.13(13)	C(12)	0.00(8)
C(2)	−0.13(13)	C(13)	0.05(8)
C(3)	−0.09(9)	C(14)	−0.14(8)
C(4)	0.07(7)	C(15)	0.06(8)
C(5)	0.00(7)	C(16)	−0.01(8)
C(6)	−0.08(7)	C(17)	0.07(8)
C(7)	0.06(7)	C(18)	−0.02(8)

transferring charge from each side of the molecule as one would expect. A ring (3, +1) critical point was located at the center of the ring, positioned at 1.439, 1.398, 1.389, 1.406, 1.396, and 1.406 Å from atoms C(4), C(5), C(6), C(7), C(8), and C(9), respectively. The local depletion of charge at this center ($\nabla^2\rho = 3.7$) is typical for such an environment.

In common with the C(3) site, a substantial amount of π electron density surrounds the C(10) atom, judging by the ellipticity values. The ellipticity value for the bond C(7)-C(10), implies that C(10) is conjugated with the phenyl ring. Such a level of conjugation represents the presence of a fair degree of the quinoidal state in the molecule. The slightly higher ellipticity values for the N(3)-C(10) and N(4)-C(10) bonds and the very high level of local charge concentration in these bonds, as deduced from the highly negative $\nabla^2\rho$ values and Fig. 4(c), indicate that N(3) and N(4) are involved in stabilizing the formal positive charge in the zwitterionic form.

In summary, electronic delocalization appears to be present throughout all of the planar component of the molecule. This shows that there must exist a fair mixture of the quinoidal and zwitterionic states in the molecule at 20 K.

B. Bond-length-alternation type calculations

1. Calculations based on the "strength-length" analogy

The level of zwitterionic: quinoidal character of DED-TCNQ was quantified previously using calculations based on the structure determined at 150 K using conventional single-crystal diffraction techniques.[2] These calculations were based on the equations

$$D^S_{\mathrm{TCNQ}} = \sum_{i=1}^{N_b} |\mathbf{b}_i^s - \mathbf{b}_i^{\mathrm{TCNQ}}| / \mathbf{N}_b , \tag{7}$$

$$\chi_s = [(D^{\mathrm{zwit}}_{\mathrm{TCNQ}} - D^S_{\mathrm{TCNQ}}) / D^{\mathrm{zwit}}_{\mathrm{TCNQ}}] \times 100, \tag{8}$$

where $b_i{}^s$ is the ith bond length in structure S and $b_i{}^{\mathrm{TCNQ}}$ is the ith bond in the ideal TCNQ form. N_b is the number of bonds over which the average was derived. $D^S{}_{\mathrm{TCNQ}}$ is a measure of the average deviation in bonding character of struc-

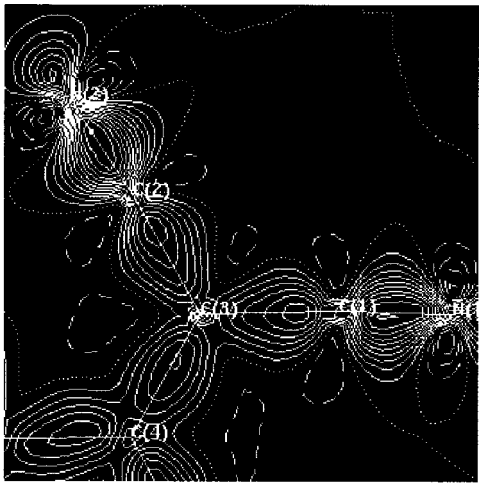

a

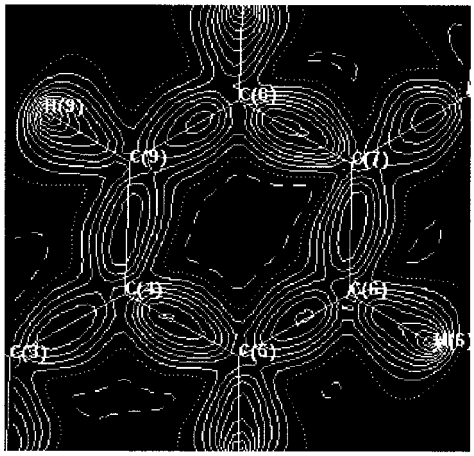

b

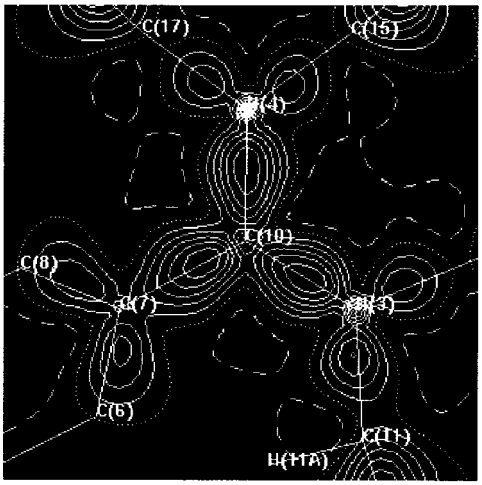

c

FIG. 4. Model electron deformation density maps for the (a) nitrile, (b) phenyl, (c) substitution point of the -C(NEt)$_2$ group in DED-TCNQ with contour levels of 0.1 e/Å. The model is calculated from the Fourier transform of the calculated structure factors. (Solid lines are positive, dashed lines are negative, and dotted lines are zero.)

TABLE V. Information regarding all bond (3, −1) critical points located within the molecule of DED-TCNQ. (λ_1, λ_2 and λ_3 are the eigenvalues of the second derivative of the electron density, ρ, at the bond critical point; $\nabla^2\rho$ is the sum of these eigenvalues; ε is the ellipticity defined as $\varepsilon=(\lambda_1-\lambda_2)/\lambda_2$; R_{ij} is the length of the bond path between the atoms; $d1$ and $d2$ represent the distance between the first and second atoms specified in the bond column and the critical point, respectively.)

Bond	λ_1	λ_2	λ_3	ρ	$\nabla^2\rho$	ε	R_{ij}	$d1$	$d2$
N(1)—C(1)	−27.70	−26.05	28.33	3.292	−25.425	0.06	1.17	0.752	0.421
N(2)—C(2)	−29.37	−28.57	31.77	3.442	−26.168	0.03	1.17	0.757	0.415
N(3)—C(10)	−19.40	−15.83	11.14	2.340	−24.091	0.23	1.34	0.794	0.549
N(3)—C(11)	−10.87	−9.99	11.98	1.629	−8.880	0.09	1.48	0.880	0.597
N(3)—C(13)	−11.93	−10.55	12.26	1.669	−10.227	0.13	1.48	0.867	0.613
N(4)—C(10)	−19.62	−15.03	10.93	2.308	−23.728	0.31	1.35	0.804	0.543
N(4)—C(15)	−10.47	−9.71	11.98	1.578	−8.202	0.08	1.48	0.871	0.608
N(4)—C(17)	−10.57	−9.85	12.73	1.590	−7.691	0.07	1.48	0.862	0.618
C(1)—C(3)	−14.10	−11.55	12.03	1.963	−13.616	0.22	1.41	0.744	0.667
C(2)—C(3)	−14.45	−12.43	12.11	2.000	−14.772	0.16	1.41	0.735	0.672
C(3)—C(4)	−13.33	−11.43	11.22	1.868	−13.552	0.17	1.44	0.739	0.704
C(4)—C(5)	−15.82	−13.79	11.26	2.113	−18.355	0.15	1.42	0.714	0.708
C(4)—C(9)	−14.18	−12.05	11.73	1.990	−14.502	0.18	1.42	0.722	0.698
C(5)—C(6)	−15.49	−12.97	10.64	2.090	−17.818	0.19	1.39	0.674	0.715
C(6)—C(7)	−15.04	−12.51	11.23	2.035	−16.324	0.20	1.41	0.717	0.693
C(7)—C(8)	−16.61	−13.68	11.25	2.167	−19.039	0.21	1.41	0.695	0.713
C(7)—C(10)	−12.61	−11.09	10.93	1.789	−12.779	0.14	1.47	0.688	0.780
C(8)—C(9)	−15.17	−12.58	10.89	2.105	−16.851	0.21	1.39	0.724	0.663
C(11)—C(12)	−9.96	−9.25	11.00	1.540	−8.215	0.08	1.52	0.791	0.734
C(13)—C(14)	−10.57	−10.43	11.42	1.644	−9.571	0.01	1.53	0.787	0.741
C(15)—C(16)	−10.70	−10.19	11.26	1.632	−9.634	0.05	1.53	0.796	0.732
C(17)—C(18)	−11.01	−9.94	11.24	1.638	−9.700	0.11	1.53	0.770	0.757

ture S compared to that in TCNQ and $D_{\mathrm{TCNQ}}^{\mathrm{ZWIT}}$ is this level of deviation in bonding character between the two extreme zwitterionic and TCNQ forms. χ_s signifies the percentage of quinoidal character that structure S possesses. In the previous study $\chi_{\mathrm{DED\text{-}TCNQ}}$ was calculated to be 27(2)%, i.e., ~3:1 zwitterionic:quinoidal in bonding character.

χ_s was recalculated using data from this study in order to (a) assess the level of validity of these previous measurements, based on the IAM rather than a multipolar model and (b) establish any temperature dependence of the relative balance in the two electronic configurations. Four values of χ_s were evaluated for this assessment: two from the IAM x-ray diffraction analysis (20 and 150 K), one from the 20 K IAM neutron diffraction data and the other from the 20 K multipolar analysis. The reference bond-length values used for TCNQ and a zwitterion were the same as those used in the previous study. Results are given in Table VI.

There is excellent agreement amongst all values derived from 20 K data, thus illustrating that such calculations do indeed produce accurate values using the IAM only and furthermore, the nature of the structural probe (x rays or neutrons) does not alter the result. The 20 and 150 K IAM results show a significant temperature dependence of $\chi_{\mathrm{DED\text{-}TCNQ}}$. The observed increase in TCNQ-like character with a decrease in temperature implies that the quinoidal electronic state is slightly more energetically favorable than the zwitterionic configuration.

2. Calculations based on bond ellipticities

The calculation of χ_s is based implicitly on the assumption of a ''strength-length'' relationship, the greater the π bonding present in a bond, the shorter the interatomic distance. Since ellipticity values give a direct ''topological'' measure of the level of π bonding present between a bond, the reevaluation of χ_s using values of ε in order to test the ''strength-length'' assumption was deemed pertinent. The calculations were the same as those given above except that b_i^s and b_i^{TCNQ} were replaced by ε_i^s and $\varepsilon_i^{\mathrm{TCNQ}}$. The reference values of ε were taken from a previous charge-density study on TCNQ (Ref. 31) where $\varepsilon=0.23$ for C(5)-C(6) and C(8)-C(9), $\varepsilon=0.11$ for C(4)-C(5), C(6)-C(7), C(7)-C(8), and C(4)-C(9), and $\varepsilon=0.17$ for C(3)-C(4) and C(7)-C(10) using the atom labeling scheme herein adopted. The reference val-

TABLE VI. Calculations of relative levels of zwitterionic versus quinoidal character present in DED-TCNQ according to different models.

Refinement model of diffraction data (probe/temperature for experiment)	D_s^{TCNQ}	χ_s(%)
IAM (x rays, 150 K)	0.038 (Ref. 2)	27(2) (Ref. 2)
IAM (x rays, 20 K)	0.034	37(2)
IAM (neutrons, 20 K)	0.032	39(2)
Multipolar (x rays, 20 K)	0.033	37(2)

ues for ε for bonds in the ring of the zwitterion extreme were taken to be $\varepsilon = 0.17$ (derived by taking the midpoint between the two different bonding types in the ring from the TCNQ-TTF reference study, $\varepsilon = 0.23 - 0.11$) and $\varepsilon = 0$ was assumed for bonds C(3)-C(4) and C(7)-C(10) since these should exhibit pure σ bonding only in this canonical form, thus having a spherical cross section of electron density between the respective bonds. The corresponding calculation of χ_s yielded a value of 44(4)% which is identical to that deduced from calculations based on the respective bond lengths at 20 K, within experimental error (the difference is just over 1 estimated standard deviation). Therefore, this confirms that the assumption of the ''strength-length'' analogy is entirely satisfactory. In addition, such consistency obtained between deductions based on bond lengths and ε values corroborates the conjecture that the results from the multipolar analysis are of a very good level of accuracy.

3. Relating bond-length-alternation type results to molecular hyperpolarizability

The 63:37 zwitterionic: quinoidal ratio lends the material good potential with respect to NLO properties since such an electronic configuration represents a BLA fairly close to the midpoint between the cyanine limit (i.e., a 50:50 zwitterionic: quinoidal mix) and the entirely zwitterionic form, the BLA at this point (corresponding to a ratio of 75:25 zwitterionic: quinoidal) yielding a maximum as a function of β (see point II Fig. 1). Since β is intrinsically dependent on μ [see Eq. (1)], the ratio corresponding to the point of maximum curvature of β will vary to some extent between derivatives with different levels of conjugation and/or donor and acceptor groups, but the general profile of the function remains constant and the maximum will always lie at a BLA value in the vicinity of this midpoint. Moreover, the temperature effects of BLA observed (the zwitterionic:quinoidal ratio rising to 73:27 at 150 K) indicate that the material could, in principal, be ''temperature tuned'' so as to obtain a BLA that corresponds to the maximum point of curvature of β.

C. Calculation of molecular dipole moment from the charge-density results

Charge-density studies enable one to ascertain the values of multipolar moments in the molecule. The dipolar moment is calculated according to the equation[32,33]

$$\mu_a = \sum_{j=1}^{n} a_j (Z_j - P_c - P_v) + q_{ja}, \tag{9}$$

where a_j denotes the vector component *x*, *y*, or *z* (Cartesian frame of reference) of atom *j*, Z_j is the atomic charge on atom *j*, P_v and P_c are the valence and core populations of atom *j*, respectively, and q_j is the contribution of the dipolar moment to the overall charge distribution which is derived from the product of the integrated Slater-type radial function, the associated Legendre function and the population coefficient[32,33]

$$q_{ja} = 4 P_{jlm} (n_l + 3)!/3\kappa_j' \xi (n_l + 2)!. \tag{10}$$

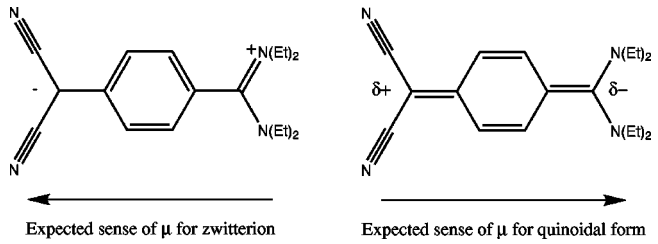

FIG. 5. The expected sense of dipole moment for a purely zwitterionic and purely quinoidal electronic configuration of DED-TCNQ.

By specifying the origin as the molecular center of mass, tensorial coefficients of $\mu_x = -23 \times 10^{-30}$ Cm, $\mu_y = -37 \times 10^{-30}$ Cm and $\mu_z = 80 \times 10^{-30}$ Cm were derived from the experimental results in this semiempirical fashion. The resulting dipolar vector lies almost directly along the molecular axis, but tilted away from the molecular plane by 27(5)°. The negative charge of the molecular dipole (the charge-transfer axis) is directed directly across the molecule, passing from the ethyl (electron donating) end towards the cyano (electron withdrawing) groups, thus corroborating the predominance of the zwitterionic molecular character (the opposite sense of μ would be expected for a molecule of wholly quinoidal character, see Fig. 5).

The near coincidence of charge-transfer and molecular axes is expected since the molecule is twofold symmetric about the molecular axis and all π-electron density lies within the molecular plane. The slight tilt of the charge-transfer axis from the molecular plane probably owes itself to strong local field effects. Indeed, the local field effects are evidently very strong given the particularly large *magnitude* of the total molecular dipole moment $|\mu| = 91 \times 10^{-30}$ Cm: this value is markedly larger than such values derived from calculations of μ in the gas and liquid phases: 33.36×10^{-30} Cm and 66.71×10^{-30} Cm, respectively.[13] Strong local field effects would also account for the otherwise surprising lack of intermolecular hydrogen bonding in this compound despite the prevalence of C-H···N nonbonded contacts in very similar materials, the terminal nitrile groups being the principal sources of hydrogen-bond acceptors. Such information on local field effects is important *a priori* information for modelling studies of these materials when included in guest-host media and for understanding the SHG properties of similar derivatives that crystallize in noncentrosymmetric space groups.

IV. CONCLUSIONS

The charge-density distribution in this important NLO precursor has been determined at 20 K and has revealed several novel results. Our previous report on a series of these TCNQ derivatives, including the subject compound, gave a bond-length-alternation type analysis which is very relevant in the field of organic non-linear optics. Such analysis is based on the basic assumption of a ''strength-length'' relationship between bonds. This work takes this analysis further by assessing whether or not such a naive approach is robust in these materials via a new topological approach to these

calculations and also if the bond-length-alternation effects are temperature dependent. By the careful combination of 20 K x-ray and neutron diffraction data and extensive crystallographic modelling, using a multipole formalism, the ''strength-length'' approach is shown to be valid in these derivatives, and is also found to be temperature dependent.

The topological approach exploits the ellipticity of the bonding density that is derived from the charge-density study. The remarkable agreement between the experimental measures of *size* (bond lengths) and *shape* (electron density of the bond cross sections) is very encouraging and is illustrative of the high regard that one can place upon the intrinsic structure/property relationships in organic nonlinear optics. The observed sensitivity of the bond-length-alternation type calculations to temperature corroborates the fact the quinoidal and zwitterionic electronic configurations lie very close in energy and also indicates the quinoidal form is the more thermally stable.

In addition, this charge-density analysis also yields important information regarding the relative polarization of electron density throughout the molecule. We have been able to partition this electronic distribution to isolate pseudocharges on each atom and, from these, determine the level and detailed nature of the molecular charge transfer that dominates β (the cause of the NLO effect on a molecular scale). In addition, such partitioning has allowed us to determine the magnitude and direction of the molecular dipole moment in the solid state. The deduction of this property in the solid state, and in particular its sense, is very difficult by any other technique. The results show that local crystal field effects strongly affect the environment in the solid state. Given the inherent link of local field effects to the molecular (β) and macroscopic ($\chi^{(2)}$) NLO origins, this information is important preliminary information for investigations of the NLO effects of these precursors when poled within an inert host matrix.

ACKNOWLEDGMENTS

The authors wish to thank the Institut Laue Langevin, Grenoble, France (J.M.C.), St. Catharine's College, Cambridge (J.M.C.), and the EPSRC (J.A.K.H. and M.S.) for financial support.

*Author for correspondence. Present address: Department of Chemistry, University of Cambridge, Lensfield Road, Cambridge, CB2 1EW. UK. E-mail: jmc61@cam.ac.uk

†Present address: CASS, SmithKline Beecham, NFSP(N), 3rd Avenue, Harlow, Essex, SM19 5AW, UK.

[1] J. C. Cole, J. A. K. Howard, G. H. Cross, and M. Szablewski, Acta Crystallogr., Sect. C: Cryst. Struct. Commun. **51**, 715 (1995).

[2] J. C. Cole, J. M. Cole, G. H. Cross, M. Farsari, J. A. K. Howard, and M. Szablewski, Acta Crystallogr., Sect. B: Struct. Sci. **53**, 812 (1997).

[3] J. M. Cole, Ph.D. thesis, University of Durham, UK, 1997.

[4] M. Szablewski, P. R. Thomas, A. Thornton, D. Bloor, G. H. Cross, J. M. Cole, J. A. K. Howard, M. Malagoli, F. Meyers, J.-L. Bredas, W. Wenseleers, and E. Goovaerts, J. Am. Chem. Soc. **119**, 3144 (1997).

[5] M. Ravi, M. Szablewski, N.-A. Hackman, G. H. Cross, D. Bloor, A. E. Goeta, and J. A. K. Howard, New J. Chem. **23**, 841 (1999).

[6] S. R. Marder, C. B. Gorman, L. Cheng, and B. G. Tiemann, Proc. SPIE **1775**, 19 (1993).

[7] C. B. Gorman and S. R. Marder, Proc. Natl. Acad. Sci. U.S.A. **90**, 11297 (1993).

[8] F. Meyers, S. R. Marder, B. M. Pierce, and J.-L. Bredas, J. Am. Chem. Soc. **116**, 10703 (1994).

[9] J. L. Oudar and D. S. Chemla, J. Chem. Phys. **66**, 2664 (1977).

[10] B. F. Levine and C. G. Bethea, J. Chem. Phys. **66**, 1070 (1977).

[11] S. J. Lalama and A. F. Garito, Phys. Rev. A **20**, 1179 (1979).

[12] W. G. Cady, *Piezoelectricity* (McGraw-Hill, New York, 1946).

[13] P. R. Thomas, Ph.D. thesis, University of Durham, UK, 1998.

[14] J. Zyss and J. L. Oudar, Phys. Rev. A **26**, 2028 (1982).

[15] D. M. Burland, R. D. Miller, and A. Walsh, Chem. Rev. **94**, 31 (1994).

[16] W. R. Hertler, H. D. Hartzler, D. S. Acker, and R. E. Benson, J. Am. Chem. Soc. **84**, 3387 (1962).

[17] R. C. B. Copley, A. E. Goeta, C. W. Lehmann, J. C. Cole, D. S. Yufit, J. A. K. Howard, and J. M. Archer, J. Appl. Crystallogr. **30**, 413 (1997).

[18] M. S. Lehmann and F. K. Larsen, Acta Crystallogr., Sect. A: Cryst. Phys., Diffr., Theor. Gen. Crystallogr. **30**, 580 (1974).

[19] R. H. Blessing, J. Appl. Crystallogr. **19**, 412 (1986).

[20] C. Wilkinson, H. W. Khamis, R. F. D. Stansfield, and G. J. McIntyre, J. Appl. Crystallogr. **21**, 471 (1988).

[21] P. Coppens, in *Crystallographic Computing*, edited by F. R. Ahmed (Munksgaard, Copenhagen, 1970).

[22] G. M. Sheldrick, SHELXL-93: *Program for the Refinement of Crystal Structures using Single Crystal Diffraction Data*, University of Göttingen, Germany, 1993.

[23] T. Koritsankszky, S. Howard, T. Richter, P. R. Mallinson, Z. Su, and N. Hansen, *A Computer Program Package for Multipole Refinement and Analysis of Charge Densities from Diffraction Data*, Berlin, 1994.

[24] R. F. Stewart, Isr. J. Chem. **16**, 124 (1977).

[25] E. Clementi and D. L. Raimondi, J. Chem. Phys. **38**, 2686 (1963).

[26] N. K. Hansen and P. Coppens, Acta Crystallogr., Sect. A: Cryst. Phys., Diffr., Theor. Gen. Crystallogr. **34**, 909 (1978).

[27] R. F. Stewart, E. R. Davidson, and W. T. Simpson, J. Chem. Phys. **42**, 3175 (1965).

[28] R. H. Blessing, Acta Crystallogr., Sect. B: Struct. Sci. **51**, 816 (1995).

[29] F. L. Hirshfeld, Acta Crystallogr., Sect. A: Cryst. Phys., Diffr., Theor. Gen. Crystallogr. **32**, 239 (1976).

[30] F. W. Bader, *Atoms in Molecules. A Quantum Theory* (Clarendon, Oxford, 1994).

[31] E. Espinosa, E. Molins, and C. Lecomte, Phys. Rev. B **56**, 1820 (1997).

[32] M. A. Spackman, Chem. Rev. **92**, 1769 (1992).

[33] T. Koritsanszky, S. Howard, P. R. Mallinson, Z. Su, T. Richter, and N. K. Hansen, XD. *A computer program package for multipole refinement and analysis of charge densities from diffraction data*, 1995.